Detection of a Thousand Copies of miRNA without Enrichment or Modification

ARTICLE *in* ANALYTICAL CHEMISTRY · JUNE 2012

Impact Factor: 5.64 · DOI: 10.1021/ac301546p · Source: PubMed

5 AUTHORS, INCLUDING:

David Wegman
York University
10 PUBLICATIONS **105** CITATIONS
SEE PROFILE

Sergey N Krylov
York University
167 PUBLICATIONS **3,624** CITATIONS
SEE PROFILE

analytical chemistry

Letter

pubs.acs.org/ac

Detection of a Thousand Copies of miRNA without Enrichment or Modification

Bryan J. Dodgson,[†] Amir Mazouchi,[‡] David W. Wegman,[†] Claudiu C. Gradinaru,*[,‡] and Sergey N. Krylov*[,†]

[†]Department of Chemistry and Centre for Research on Biomolecular Interactions, York University, Toronto, Ontario M3J 1P3, Canada

[‡]Department of Physics, University of Toronto and Department of Chemical and Physical Sciences, University of Toronto Mississauga, Mississauga, Ontario L5L 1C6, Canada

Supporting Information

ABSTRACT: We report direct quantitative analysis of multiple miRNAs with a detection limit of 1000 copies without miRNA enrichment or modification. A 300-fold improvement over the previously published detection limit was achieved by combining capillary electrophoresis with confocal time-resolved fluorescence detection through an embedded capillary interface. The method was used to determine levels of three miRNA biomarkers of breast cancer (miRNA 21, 125b, 145) in a human breast cancer cell line (MCF-7). A 30 pL volume of the cell lysate with approximately a material content of a single cell was sampled for the analysis. MiRNA 21, which is up-regulated in breast cancer, was detected at a level of approximately 12 thousand copies per cells. MiRNAs 125b and 145, which are down-regulated in breast cancer, were below the 1000-copy detection limit. This sensitive method may facilitate the analysis of miRNA in fine-needle-biopsy samples and even in single cells without enrichment or modification of miRNA. Advantageously, the instrumental setup developed here can be reproduced by others as it requires no sophisticated custom-made parts.

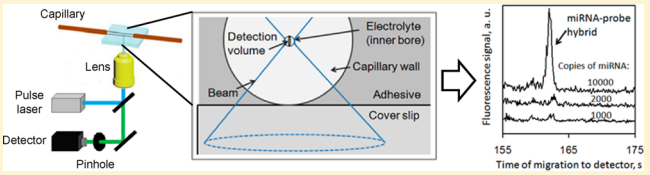

MicroRNAs (miRNAs) are short, noncoding RNA molecules (18−25 nucleotides) that participate in the regulation of the majority of cellular processes.[1] Various diseases have been associated with altered expression patterns of multiple miRNAs.[2] A significant research effort is currently focused on identifying panels of miRNA biomarkers that could serve for early disease diagnosis as well as for assessing the prognosis and monitoring the response to treatment. The efficient use of miRNA-biomarker panels requires accurate quantitative analyses of multiple miRNAs. Most available methods of miRNA detection are indirect (e.g., quantitative reverse-transcriptase polymerase chain reaction, microarrays, surface plasmon resonance, next generation sequencing, isothermal ramification amplification, etc.); they require chemical or enzymatic modifications of miRNA prior to the analysis.[3] Modifications make the analysis cumbersome and lead to reduced accuracy due to different efficiencies of modifications for different miRNAs.[4] A few direct methods, which do not require any modification of the target miRNA, are available: Northern blotting, signal amplifying ribozymes, in situ hybridization, bioluminescence detection, and two-probe single-molecule fluorescence.[5] Northern Blots using LNA probes have significantly improved sensitivity; however, they only were able to detect a single miRNA. Signal amplifying ribozymes have been used to detect nucleic acids at subzeptomolar range and have been used to detect miRNA; however, it would be difficult and cumbersome to multiplex, having to develop a new ribozyme for each miRNA target. In situ hybridization assays have been used to detect single copies of miRNAs; however, they become semiquantitative when the copy number exceeds 1000 making it difficult to be used in any biomarker assay. Bioluminescence and two-probe single-molecule fluorescence methods are both quantitative; however, they could hardly be used for detecting multiple miRNAs.

Direct quantitative analysis of multiple miRNAs (DQAMmiR) has been recently developed upon a classical hybridization approach (in which hybridization probes, labeled for detection and taken in excess to miRNAs, bind miRNAs sequence-specifically, and unreacted probes are separated from the probe−target hybrids by electrophoresis) (Figure 1).[6] Capillary electrophoresis (CE) with laser-induced fluorescence (LIF) detection had been successfully used in direct hybridization analysis of a single miRNA[7] and was, thus, chosen as an instrumental platform for DQAMmiR. The challenging problems of electrophoretic separation of (i) the excess probes (single strand DNA) from the probe−miRNA hybrids and (ii) the hybrids from each other were solved through the combined use of single strand DNA binding (SSB) protein in the run buffer[8] and drag tags on the probes.[9] The limit of detection of DQAMmiR (which is defined as a number of copies of miRNA

Received: June 5, 2012
Accepted: June 8, 2012
Published: June 8, 2012

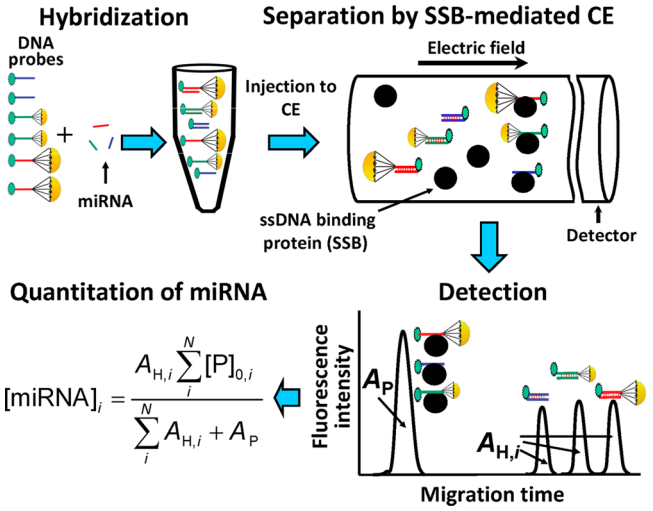

Figure 1. Schematic representation of the direct quantitative analysis of multiple miRNAs (DQAMmiR) by CE. miRNAs and their complementary ssDNA probes are shown as short lines of the same color, drag tags are shown as parachutes, a fluorescent label is shown as small green circles, and ssDNA-binding protein (SSB) is shown as large black circles. In the hybridization step, the excess of the probes of concentrations $[P]_{0,i}$ is mixed with the miRNAs which leads to all miRNAs' being hybridized but with some probes left unbound. A short plug of the hybridization mixture is introduced into a capillary prefilled with an SSB-containing run buffer. SSB binds all ssDNA probes but does not bind the double stranded miRNA-DNA hybrid. When an electric field is applied, all SSB-bound probes move faster than all the hybrids (SSB works as a propellant).[8] Different drag tags make different hybrids move with different velocities. SSB-bound probes, however, can move even with similar velocities if the drag tags are small with respect to SSB. In such a case, a fluorescent detector at the end of the capillary generates separate signals for the hybrids and a cumulative signal (one peak or multiple peaks) for the excess of the probes. The amounts (or concentrations) of miRNAs are finally determined with a simple mathematical formula that uses the integrated signals (peak areas in the graph: $A_{H,i}$ for the areas corresponding to the hybrids and A_P for the total area corresponding to the unbound probes). Adapted with permission from ref 6. Copyright 2011 John Wiley & Sons, Inc.

that corresponds to a peak with a signal-to-noise ratio, S/N, equal to 3) was in the order of 3×10^5 copies of miRNA in a consumed sample, and this was achieved with arguably the most sensitive CE-LIF instrument commercially available. The relatively poor limit of detection imposes an important restriction on this otherwise powerful analytical technique: DQAMmiR may be inapplicable to measuring miRNAs in fine-needle aspiration biopsies, which became standard in diagnosis of cancer and other diseases.[10] Indeed, fewer than 1000 copies of miRNA may be present in a cell, and fine-needle biopsies typically contain in the order of 100 cells. The total number of miRNA copies in such a sample would be less than 10^5, which is below the current limit of detection of DQAMmiR. The goal of this work was to find a way for improvement in the detection limit of DQAMmiR which would make it applicable to small numbers of cells while keeping it simple and practical for easy use by life scientists and medical researchers. We chose ~1000 copies of miRNA as an intended detection limit of DQAMmiR, as it would guarantee the analysis of most miRNA is a sample of ~100 cells (typical for fine-needle aspiration biopsy).

The limit of detection of DQAMmiR depends on two factors: the efficiency of hybridization/separation and the fluorescence detection efficiency (see Figure 1). While both efficiencies can be improved, the detection efficiency promised the largest gain as the limit of detection of pure fluorophore was found to be only ~10 times better than that of miRNA (see Supporting Information). Therefore, we focused on identifying inherent problems of fluorescence detection in CE and finding a solution that (i) would offer a DQAMmiR limit of detection of ~1000 copies of miRNA (or ~1000/10 = ~100 copies of pure fluorophore) and (ii) would be achievable with a robust and easy-to-operate instrumental setup built of commercial parts (without sophisticated custom-made components) and utilizing ordinary round capillaries.

CE-LIF is a mature technique with many custom-made and commercial fluorescence detectors developed over the last 2 decades. The major reason for poor detection limit is the presence of background in a fluorescence signal from 3 major sources: (i) Rayleigh light scattering from capillary walls (at the laser wavelength), (ii) Raman light scattering on water (red-shifted compared to the laser wavelength), and (iii) autofluorescence from the capillary walls. The issue of background was systematically addressed by a number of groups, and outstanding limits of detection were achieved in 3 approaches. The first approach utilizes postcolumn detection by means of a custom-made sheath-flow cuvette and allows detection of ~10 molecules of sulforhodamine 101 (a pure fluorophore) in its best implementation.[11] The second approach uses custom-pulled capillaries with a narrow inner diameter (~2 μm) and thin capillary wall (~25 μm); it allows for single molecule detection within a capillary while having a concentration limit of detection in the subpicomolar range for fluorescein (3000 molecules at 10 nL of injection).[12] Finally, the third approach replaces round capillaries with rectangular channels in custom-made microfluidic chips which allows detection of individual fluorophore molecules with over 90% efficiency in best instances.[13] While facilitating detection limits suitable for DQAMmiR, these approaches do not satisfy the requirement of simplicity: they all involve custom-made parts that are difficult to reproduce and/or operate. Thus, we sought an approach to reduce light scattering and background fluorescence, which would use on-column detection with a commercial round capillary and would not involve sophisticated custom-made parts.

In general, background from light scattering and undesirable fluorescence can be reduced by photon-counting detection and by three types of signal filtering: (i) spectral, (ii) spatial, and (iii) temporal. Spectral filtering utilizes a combination of cutoff and band-pass filters that allow only light within a spectral range of the fluorophore's emission to reach the detector. Spatial filtering uses an aperture to reject stray light from outside the region of interest; it is most effectively achieved using confocal optics to define a 3-D detection volume. Finally, time-resolved fluorescence (TRF) measurements can facilitate temporal filtering to gate-out scattering by monitoring the time delay of detected photons following excitation pulses. Ultimate reduction of background in CE-LIF requires the combination of all 3 filtering approaches. While spectral filtering is used in all setups by default, to the best of our knowledge, a combination of confocal and TRF detection has only been used in CE for lifetime measurements[14] and for detection of proteins with an estimated detection limit of ~10^4–10^5 molecules.[15] Thus, the theoretical potential of the combined confocal/TRF (CTRF) approach has never been utilized or even experimentally confirmed for CE. The goal of our work was to fill out this gap

dx.doi.org/10.1021/ac301546p | Anal. Chem. 2012, 84, 5470–5474

and, if proved successful, to use the CTRF approach for improving the detection limit of DQAMmiR.

A part of our team has developed an advanced CTRF setup that could serve as a prototype detector for CE without any modification (Figure 2, lower part). The detector is described

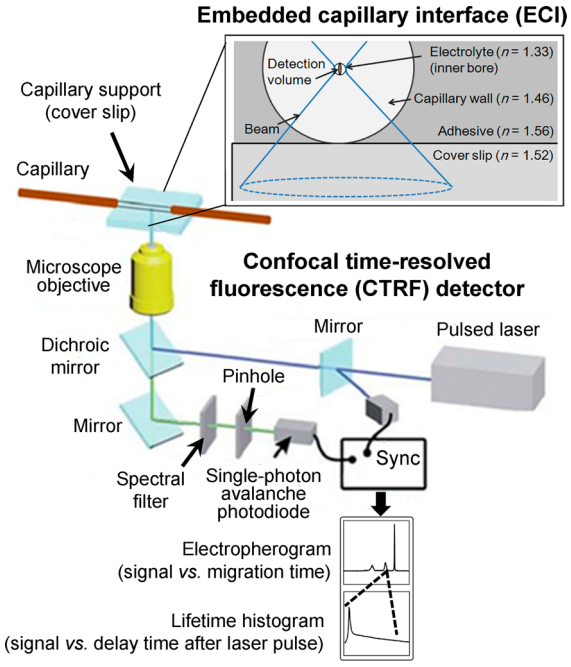

Figure 2. Schematic of a setup for confocal time-resolved fluorescence (CTRF) detection through an embedded capillary interface (ECI). See text for details.

in detail elsewhere;[16] here, we briefly outline its major components, principles of operation, and characteristics. The beam from a pulsed femtosecond laser is shaped and directed onto a high numerical aperture objective, which both delivers excitation light to the sample and collects a large fraction of the emitted fluorescence. The collected light is passed through spectral filters and a pinhole to allow for confocal detection. Single-photon avalanche diode (SPAD) detectors and time-correlated single photon counting electronics are used to record the time interval between excitation and detection ("microtime") as well as the absolute detection time ("macrotime") for each photon.

In experiments, the fluorescence intensity-time trajectory and lifetime histogram are simultaneously constructed on the basis of photon timings recorded on the same data set. The intensity-time trajectory (electropherogram) is obtained by binning photons according to their macrotime tag, typically in 100 ms bins in a trace lasting several minutes. Histograms of photon microtimes yield the fluorescence decay in 4 ps steps over a 12.5 ns range. The resolution of lifetime measurements is determined by the width of the instrument response function of the SPAD detector, 44 ps.

With this highly sensitive setup, single fluorescent molecules can be detected reliably without a capillary as they diffuse through the confocal detection volume.[16] The sensitivity of this design is due to the combination of high-efficiency light collection with efficient spatial and spectral filtering. In the original design, the multiparameter detection, including TRF, was intended for the study of single molecule dynamics in complex environments and for fluorescence lifetime imaging microscopy.[17] However, TRF was also efficiently employed to improve the signal-to-noise ratio in correlation fluorescence spectroscopy measurements by gating-out photons with microtimes less than 0.5 ns. This type of data filter suppresses the coherent signals, e.g., scattering, and for most practical cases, reduces the incoherent signals, e.g., fluorescence, only very slightly. Therefore, ultrasensitive in-capillary measurements should become possible provided that we can maintain high optical collection efficiency by properly interfacing the objective with the capillary.

Interfacing the objective lens with the capillary requires a proper thickness (~170 μm) of glass material with the appropriate optical characteristics (borosilicate glass, n = 1.52) so that significant spherical aberrations are avoided. In addition, the focal point should be set to the optimum depth (~5 μm) into the liquid sample to minimize the induced aberration due to optical mismatch between the oil objective and aqueous sample.[16] The design of the interface must also satisfy the requirement of needing no sophisticated custom-made parts. We came up with a very simple embedded capillary interface (ECI) design that satisfies these requirements (Figure 2, upper part). An ordinary round capillary (5 μm inner radius, 58 μm wall thickness) is placed on a glass support (110 μm thick microscope coverslip) and simply glued to its surface with an optical adhesive that has a refractive index (1.56) closely matching those of the glass materials of the capillary (1.46) and the support (1.52). The design also matches the thickness of glass between the lens and the capillary core (168 μm) with the thickness of a standard coverslip, for which the objective has been corrected (~170 μm). Finally, the preparation of ECI takes only a few minutes and requires no specific skills or sophisticated equipment. The ECI is mounted on a 3-axis piezo scanner which controls the position (X and Y directions) and depth of focus into the ECI (Z direction) with subnanometer resolution.

We use the abbreviation of CE-CTRF-ECI for capillary electrophoresis with confocal time-resolved fluorescence detection through an embedded capillary interface. To facilitate the proof-of-principle experiments, we used a basic CE setup in which the ends of the capillary were inserted into two small vials with an electrolyte (25 mM sodium tetraborate) and an electric field (300 V/cm) was applied through two platinum electrodes. The sample was injected into the capillary by pressure (a more detailed description of the CE-CTRF-ECI is in the Supporting Information).

The limit of detection of CE-CTRF-ECI was assessed by sampling serial dilutions of fluorescein (Figure 3A). For each measurement, 60 pL of the dye solution was injected into the capillary and S/N of each electrophoretic peak was measured. The dependence of S/N on the number of sampled molecules of fluorescein was linear, and a S/N ≈ 3 was obtained for 3 pM fluorescein. Thus, the detection limit was estimated to be ~100 dye molecules. This result is even more remarkable, considering that approximately only ~10% of these molecules pass through the detection volume (see Supporting Information). A closer match between the axial cross section of the detection volume and the diameter of the capillary inner bore can potentially improve the sensitivity by approximately an order of magnitude. To test the robustness of the system, the assembly of the ECI on the microscope was repeated several times over a 3 month period. The reported limit of detection was achieved in all experiments. The detection limit of CE-CTFR-ECI meets the detection limit requirement of 100 molecules (of pure

dx.doi.org/10.1021/ac301546p | Anal. Chem. 2012, 84, 5470−5474

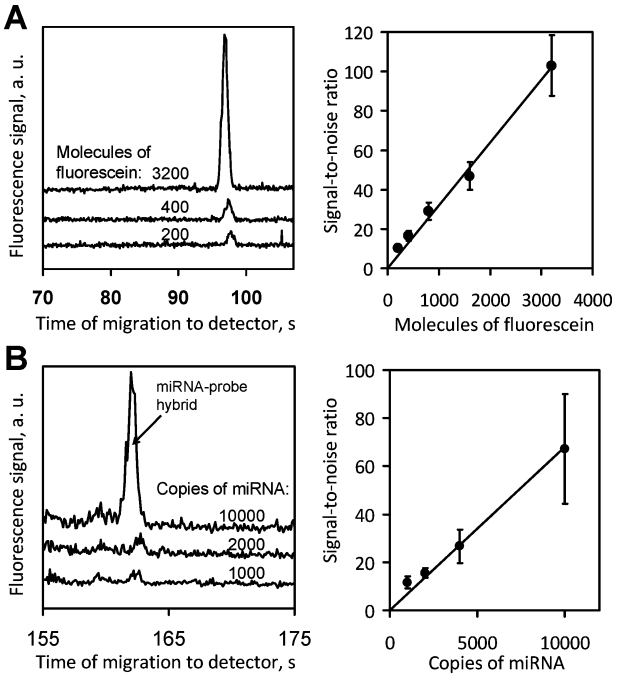

Figure 3. Limit of detection of CE-CTRF-ECI for the analysis of: a pure fluorophore, fluorescein (A), and miRNA (miRNA 21 as an example) by DQAMmiR (B). The left panels show electropherograms (offset along the Y axis for clarity of presentation) while the right panel shows the dependence of the signal-to-noise ratios on the number of molecules in the sample.

fluorophore) that we set as a goal. It is also ~2 orders of magnitude better than the best reported value for detection inside ordinary round capillaries.[18]

We then measured the detection limit of our DQAMmiR analysis performed with CE-CTFR-ECI (Figure 3B). A previously developed protocol for DQAMmiR was slightly modified: concentrations of miRNA and probes were decreased, and the incubation time was increased. Three synthetic RNA oligonucleotides (identical to miRNA 21, 125b, and 145, which are known breast cancer biomarkers) were prepared at varying concentrations and sampled for DQAMmiR. The S/N was calculated for each experiment and plotted against the number of sampled molecules of miRNA. We found that samples with 1000 copies of either miRNA led to an electrophoretic peak with S/N $\geq$ 3. The errors of the plot in Figure 3B are higher than those in Figure 3A due to a combination of hybridization and separation errors in Figure 3B. The plot in Figure 3B slightly deviates from linearity most likely due to a small systematic error in the relatively complex hybridization assay. The relatively high errors in both S/N plots in Figure 3 are associated with the nature of S/N measurements that combine errors of both signal and noise.

The hybrid peak was preceded by increased noise associated with impurity present in the probe. The impurity noise was always baseline-separated from the hybrid peak and did not interfere with hybrid detection. Thus, the detection limit of DQAMmiR performed with CE-CTRF-ECI was 1000 copies of miRNA. This is 300 times better than the detection limit achieved with a commercial CE instrument with arguably the most sensitive on-column LIF detector.[6] In a clinical setting, the limit of quantification (S/N = 10) provides a more appropriate limit on the number of copies that can be accurately detected; this limit corresponds to roughly 3000 copies.

Finally, we applied DQAMmiR performed with CE-CTRF-ECI to the analysis of the 3 miRNAs in MCF-7 breast cancer cells (Figure 4, lower trace). The hybridization mixture was

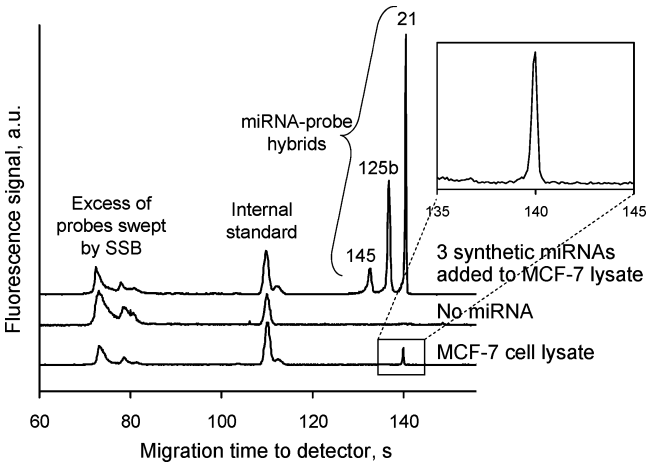

Figure 4. Analysis of 3 miRNAs (miRNA 145, 125b, and 21) by DQAMmiR using the CE-CTRF-ECI setup. The upper trace corresponds to sampling a mixture of 3 synthetic miRNAs in MCF-7 lysate (positive control). The middle trace corresponds to a sample with no miRNAs (negative control). The bottom trace corresponds to sampling the MCF-7 cell lysate; the inset shows the zoomed-in peak corresponding to 12 thousand copies of the miRNA 21–probe hybrid. Note that, despite the difference in peak heights on the top trace, the area of the three miRNA hybrids are comparable when normalized by migration time. The 3 traces are offset along the Y axis for clarity of presentation.

prepared with a crude cell lysate and 30 pL of this mixture was sampled for CE-CTRF-ECI. The use of cell lysate changes the conductivity of the sample and affects the migration times of analytes (with respect to Figure 3). However, by incorporating an internal standard, fluorescein, the time axis can be properly scaled to allow for inter-run comparisons. The internal standard also helps to account for variations in the volume of injected sample. The volume sampled was estimated to contain the cellular content of approximately 1 cell (0.8). The probe–target hybrid for miRNA 21, which is up-regulated in these cells, was detected and corresponds to 12 000 copies of miRNA 21 per cell. The signals from miRNA 125b and 145, which are down-regulated in these cells,[2b] were below the 1000 copy detection limit. The results obtained are in agreement with the previous estimates by other methods.[19]

To conclude, we were able to improve the detection limit of DQAMmiR by more than 2 orders of magnitude, which makes the method applicable to biological samples containing a small number of cells such as fine-needle aspiration biopsies. It can potentially be used for analysis of miRNA in single cells. This improvement was achieved solely by developing highly sensitive CE-CTRF-ECI, which advantageously combines spectral, spatial, and temporal photon filtering. Despite using an ordinary round glass capillary and an extremely simple capillary-optics interface, CE-CTRF-ECI has a detection limit of 100 molecules of pure fluorophore. Importantly, this approach has a potential for further improvement in the detection limit without complicating the interface, by optimizing the excitation and collection optics for in-capillary

dx.doi.org/10.1021/ac301546p | Anal. Chem. 2012, 84, 5470–5474

detection. CE-CTRF-ECI shifts the onus of achieving low detection limits from custom-designing capillary-optics interfaces to assembling commercially available optics and electronics. This makes the experimental setup not only feasible for production but also robust in operation. We foresee that CE-CTRF-ECI will become a practical instrumental platform for highly sensitive analyses of miRNAs and other disease biomarkers.

■ ASSOCIATED CONTENT

Supporting Information

Additional information as noted in text. This material is available free of charge via the Internet at http://pubs.acs.org.

■ AUTHOR INFORMATION

Corresponding Author

*E-mail: claudiu.gradinaru@utoronto.ca (C.C.G.); skrylov@yorku.ca (S.N.K.).

Notes

The authors declare no competing financial interest.

■ ACKNOWLEDGMENTS

B.J.D. and A.M. contributed equally to this manuscript. The work was funded by the Natural Sciences and Engineering Research Council of Canada.

■ REFERENCES

(1) Aguda, B. D.; Kim, Y.; Piper-Hunter, M.; Friedman, A.; Marsh, C. B. *Proc. Natl. Acad. Sci. U.S.A.* **2008**, *105*, 19678−19683.

(2) (a) Visone, R.; Rassenti, L. Z.; Veronese, A.; Taccioli, C.; Costinean, S.; Aguda, B. D.; Volinia, S.; Ferracin, M.; Palatini, J.; Balatti, V.; Alder, H.; Negrini, M.; Kipps, T. J.; Croce1, C. M. *Blood* **2009**, *114*, 3872−3879. (b) Iorio, M. V.; et al. *Cancer Res.* **2005**, *65*, 7065−7070. (c) Michael, M. Z.; O' Connor, S. M.; van Holst Pellekaan, N. G.; Young, G. P.; James, R. J. *Mol. Cancer Res.* **2003**, *1*, 882−891.

(3) (a) Lao, K.; Xu, N. L.; Yeung, V.; Chen, C.; Livak, K. J.; Straus, N. A. *Biochem. Biophys. Res. Commun.* **2006**, *343*, 85−89. (b) Liu, C.-G.; Calin, G. A.; Meloon, B.; Gamliel, N.; Sevignani, C.; Ferracin, M.; Dumitru, C. D.; Shimizu, M.; Zupo, S.; Dono, M.; Alder, H.; Bullrich, F.; Negrini, M.; Croce, C. M. *Proc. Natl. Acad. Sci. U.S.A.* **2004**, *101*, 9740−9744. (c) Fang, S.; Lee, H. J.; Wark, A. W.; Corn, R. M. *J. Am. Chem. Soc.* **2006**, *128*, 14044−14046. (d) Morin, R. D.; O' Connor, M. D.; Griffith, M.; Kuchenbauer, F.; Delaney, A.; Prabhu, A.-L.; Zhao, Y.; McDonald, H.; Zeng, T.; Hirst, M.; Eaves, C. J.; Marra, M. A. *Genome Res.* **2008**, *18*, 610−621. (e) Yao, B.; Li, J.; Huang, H.; Sun, C.; Wang, Z.; Fan, Y.; Chang, Q; Li, S; Xi, J. *RNA* **2009**, *15*, 1787−1794.

(4) (a) Ohtsuka, E.; Nishikawa, S.; Fukomoto, R.; Tanaka, S.; Markham, A. F.; Ikehara, M.; Sugiura, M. *Eur. J. Biochem.* **1977**, *81*, 285−291. (b) McLaughlin, L. W.; Romaniuk, E.; Romaniuk, P. J.; Neilson, T. *Eur. J. Biochem.* **1982**, *125*, 639−643. (c) Weiss, E. A.; Gilmartin, G. M.; Nevins, J. R. *EMBO J.* **1991**, *10*, 215−219.

(5) (a) Varallyay, E.; Burgyan, J.; Havelda, Z. *Nat. Protoc.* **2008**, *3*, 190−196. (b) Vaish, N. K.; Jadhav, V. R.; Kossen, K.; Pasco, C.; Andrews, L. E.; Mcswiggen, J. A.; Polisky, B.; Siewart, S. D. *RNA* **2003**, *9*, 1058−1072. (c) Dore, K.; Dubus, S.; Ho, H.-A.; Levesque, I; Brunette, M.; Corbeil, G.; Boissinot, M.; Boivin, G.; Bergeron, M. G.; Boudreau, D.; Leclerc, M. *J. Am. Chem. Soc.* **2003**, *126*, 4240−4244. (d) Hartig, J. S.; Grune, I.; Najafi-Shoushtari, S. H.; Famulok, M. *J. Am. Chem. Soc.* **2004**, *126*, 722−723. (e) Obernosterer, G.; Martinez, J.; Alenius, M. *Nat Protoc.* **2007**, *2*, 1508−1514. (f) Silahtaroglu, A. N.; Nolting, D.; Dyrskjøt, L.; Berezikov, E.; Møller, M.; Tommerup, N.; Kauppinen, S. *Nat. Protoc.* **2007**, *2*, 2520−2528. (g) Kloosterman, W. P.; Wienholds, E.; de Bruijn, E.; Kauppinen, S.; Plasterk, R. H. A. *Nat. Methods* **2006**, *3*, 27−29. (h) Cissell, K. A.; Rahimi, Y.; Shrestha, S.; Hunt, E. A.; Deo, S. K. *Anal. Chem.* **2008**, *80*, 2319−2325. (i) Neely, L. A.; Patel, S.; Garver, J.; Gallo, M.; Hackett, M.; McLaughlin, S.; Nadel, M.; Harris, J.; Gullans, S.; Rooke, J. *Nat. Methods* **2006**, *3*, 41−46.

(6) Wegman, D. W.; Krylov, S. N. *Angew. Chem., Int. Ed.* **2011**, *50*, 10335−10339.

(7) Chang, P.-L.; Chang, Y.-S.; Chen, J.-H.; Chen, S.-J; Chen, H.-C. *Anal. Chem.* **2008**, *80*, 8554−8560.

(8) (a) Berezovski, M.; Krylov, S. N. *J. Am. Chem. Soc.* **2003**, *125*, 13451−13454. (b) Krylova, S. M.; Wegman, D.; Krylov, S. N. *Anal. Chem.* **2010**, *82*, 4428−4433. (c) Al-Mahrouki, A. A.; Krylov, S. N. *Anal. Chem.* **2005**, *77*, 8027−8030. (d) Khan, N.; Cheng, J.; Pezacki, J. P.; Berezovski, M. V. *Anal. Chem.* **2011**, *83*, 6196−6201.

(9) (a) Heller, C.; Slater, G. W.; Mayer, P.; Dovichi, N.; Pinto, D.; Viovy, J. L.; Drouin, G. *J. Chromatogr.* **1998**, *806*, 113−121. (b) Zhang, H.; Li, X.-F.; Le, X. C. *J. Am. Chem. Soc.* **2007**, *130*, 34−35.

(10) Roskell, D. E.; Buley, I. D. *BMJ* **2004**, *329*, 244−245.

(11) Chen, D. Y.; Adelhelm, K.; Cheng, X. L.; Dovichi, N. J. *Analyst* **1994**, *119*, 349−352.

(12) Lundqvist, A.; Chiu, D. T.; Orwar, O. *Electrophoresis* **2003**, *24*, 1737−1744.

(13) Schiro, P. A.; Kuyper, C. L.; Chui, D. T. *Electrophoresis* **2007**, *28*, 2430−2438.

(14) Lieberwirth, U.; Arden-Jacob, J.; Drexhage, K. H.; Herten, D. P.; Müller, R.; Neumann, M.; Schultz, A.; Siebert, S.; Sagner, G.; Klingel, S.; Sauer, M.; Wolfrum, J. *Anal. Chem.* **1998**, *70*, 4771−4779.

(15) Belin, G. K.; Seeger, S. *J. Nanosci. Nanotechnol.* **2009**, *9*, 2645−2650.

(16) Mazouchi, A.; Liu, B.; Bahram, A.; Gradinaru, C. C. *Anal. Chim. Acta* **2011**, *688*, 61−69.

(17) Liu, B.; Mazouchi, A.; Gradinaru, C. C. *J. Phys. Chem. B* **2010**, *114*, 15191−15198.

(18) Lee, T. T.; Yeung, E. S. *J. Chromatogr., A* **1992**, *595*, 319−325.

(19) Chan, H.-M.; Chan, L.-S.; Wong, R. N-S.; Li, H.-W. *Anal. Chem.* **2008**, *82*, 6911−6918.

Supporting Information

Detection of a Thousand Copies of miRNA without Enrichment or Modification

Bryan J. Dodgson,[1] Amir Mazouchi,[2] David W. Wegman,[1]Claudiu Gradinaru,[2] and Sergey N. Krylov[1]

[1]Department of Chemistry and Centre for Research on Biomolecular Interactions, York University, Toronto, Ontario M3J 1P3, Canada
[2]Department of Physics, University of Toronto, Department of Chemical and Physical Sciences, University of Toronto Mississauga, Mississauga, Ontario L5L 1C6, Canada

Supporting Results

Difference between the instrument detection limit and detection limit of DQAMmiR. The instrument detection limit (measured with a pure fluorophore, fluorescein) was approximately 10-fold lower (better) than the DQAMmiR detection limit. There are several reasons for this difference. While the detection of a pure fluorophore is straightforward, the detection of miRNA requires two major additional steps, hybridization and separation, that certainly affect the detection limit. The addition of the excess probe introduces impurities that add to the "noise" level. Moreover, miRNA in the sample may not be detected if it does not hybridize with the probe because of: (i) the efficiency of hybridization being less than 100%, (ii) miRNA degradation, or (iii) miRNA lost due to adsorption on surfaces (e.g. that of a sample tube). In principle, the detection limit of DQAMmiR can be improved by an order of magnitude by optimizing the efficiencies of hybridization and separation; however, this fine tuning was not the subject of this work, in which a 300-times improvement was achieved through a dramatic reduction of the fluorescence background.

Supporting materials and methods

CTRF-ECI design. The CTRF instrument included a Ti:sapphire laser (Tsunami HP, Spectra Physics, Santa Clara, CA, USA) as the excitation source, producing laser pulses of ~ 100 fs duration and 10-12 nm spectral width. The output was tuned to a center wavelength of 956 nm and frequency-doubled to 478 nm by focusing the laser beam into a β-BBO crystal. The beam was passed through a pinhole to ensure it was in the TEM_{00} mode, and a neutral density filter wheel was used for variable attenuation. A dichroic mirror directed laser light to a 1.4 NA/ 100× oil immersion microscope objective (PlanApochromat, Carl Zeiss, Toronto, Canada). The sample was placed on a cover slip fixed to the microscope stage by negatively pressurizing an empty chamber in the stage located beneath the cover slip. The microscope stage consisted of a three-way piezo-electric stage (T225, MadCity Labs, Madison, WI, USA) capable of 100 nm manipulation in the X and Y directions, and 20 nm in the Z direction. Backscattering and fluorescence was collected by the objective and passed through the dichroic mirror for filtering by long-pass and band-pass spectral filters (Semrock, Rochester, NY, USA). Light was then

passed through a 150 μm diameter pinhole aperture used for confocal detection, mounted to a three-axis micrometer translational stage. A high quantum efficiency (45%) SPAD was used as a detector (PD5CTC, Optoelectronic Components, Kirkland, Canada). The output of the SPAD and a small fraction of the laser excitation pulse, as detected by a fast photodiode (PHD-400-N, Becker & Hickl, Berlin, Germany), were used as inputs for the Time-Correlated Single-Photon Counting (TCSPC) module (PicoHarp300, PicoQuant, Berlin, Germany). This system allowed for the time-resolved detection of single photons from single fluorescent molecules, with 4 ps timing resolution, and up to a maximum count rate of 10 MHz[16, 17]

To construct the ECI device, first we created a 2 cm detection window in the capillary by removing the capillary's polyimide coating under an open flame for several seconds. The detection window and surface of the cover slip were cleaned using ethanol and the detection window was then carefully pressed to the cover slip using the plastic prongs of tweezers, which were held roughly 1 cm apart. A small bead of adhesive (NOA61, Thorlabs, Newton, NJ, USA) was placed directly in between the two prongs and the bead was cured under a UV lamp for 1 minute. The prongs were then removed and the rest of the bare capillary resting on the cover slip was coated in adhesive (to reduce fragility) and cured for 2-3 minutes.

Once the ECI was fixed to the CTRF microscope the surface of the inner bore of the capillary was determined by finding the maximum backscattering, which occurs at the glass-air interface nearest to the objective. All subsequent measurements were made with the stage translated to the centre of the capillary's inner bore (~5 μm above the surface).

We determined the size of the confocal detection volume by performing fluorescence correlation spectroscopy (FCS) measurements inside a capillary filled with a fluorophore solution. The experimentally determined autocorrelation function was best fit by a 2D diffusion model, indicating that the detection volume approximately spanned axially the full inner diameter of the capillary (10 μm). By fitting the 2-dimensional model to the data, a lateral radius of 430 nm was determined. When comparing the size of the detection volume to the dimensions of the inner diameter of the capillary, 13% of injected molecules are expected to pass through the detection volume.

To further improve S/N, the scattering is further suppressed by time-gating. A 60 pL plug of 100 pM of fluorescein was passed through the capillary by electrophoresis. The data was processed using a custom-written LabView program and the resulting electropherogram was subjected to a series of time gating window widths (within which all photons were rejected), ranging from 0 to 2.5 ns. The signal-to-noise ratio of the plug was calculated for each time-gated electropherogram and plotted as a function of gate width**.** The highest signal-to-noise ratio was achieved using a 0.5 ns gating window, which produced a 32% improvement to sensitivity relative to non-time gated data. All reported measurements employed this particular time-filter.

Experimental. Samples were injected into the capillary by negatively pressurizing an airtight chamber sealed to the outlet end of the capillary. The chamber was pressurized by drawing back the plunger on a 60 mL syringe by a pre-defined distance, for a pre-define duration of time. The exact distance and duration was controlled using an automated syringe pump (NE-1010, New Era Pump Systems Inc., Farmingdale, NY, USA). The total amount of sample injected was determined by experimentally measuring the flow rate of a fluorescent dye under the pre-defined injection pressure. Electrophoresis was carried out by placing a platinum electrode in the inlet and outlet vials and using a high voltage power supply (CZE1000r Spellman, Hauppauge, NY, USA) to provide an electric field of 300 V/cm across the capillary's length. The total length of

the capillary was 50 cm and the length from the injection end to the detection point was 7 cm. The uncertainty on the limit of detection of fluorescein was plus or minus 15% (one standard deviation), as determined by measuring the variations in area from a 60 pL injection of 100 pM of fluorescein over ten different experimental runs.

We performed the CE-based DQAMmiR method by following the sample preparation procedures previously described in "Wegman, D. W.; Krylov, S. N. Direct quantitative analysis of multiple miRNAs (DQAMmiR). *Angew. Chem. Int. Edit.* **2011**, *50*, 10335-10339." Hybridization was achieved as follows: in incubation buffer (50 mM Tris-Ac, 50 mM NaCl, 10 mM EDTA, pH 7.8), single-stranded DNA probes for the three respective miRNAs were incubated at a concentration of 5 nM (**Fig. 3B**) or 500 pM (**Fig. 4**) with the sample of interest (i.e. 2.72×10^7 cells/ml cell lysate, or spiked miRNA). Also included in the mixture was 100 pM fluorescein, 250 nM masking DNA (20-nucleotide DNA strand, AP1R) and 100 nM masking RNA (tRNA library). An internal standard, fluorescein, was added to the sample to account for variations in the volume of injected sample and changes in peak migration times in the analyses of cell lysate. The masking DNA and RNA were added to prevent the degradation of DNA and RNA, respectively, as well as to prevent adsorption of the probe or the miRNA to the walls of the vial during incubation. Pre-existing DNA or RNA structures were denatured by raising the temperature of the mixture to 80°C, and hybridization was promoted by cooling the mixture to 37°C at a rate of 20°C/min. The mixture was incubated at 37°C overnight to ensure complete hybridization without optimizing the hybridization time. To determine the microRNA detection limit, a single DNA probe-microRNA pair was used and SSB was removed from the run buffer. This was done to make it simpler to optimize the other experimental parameters. The uncertainty on the limit of detection of microRNA was plus or minus 20% (one standard deviation), as determined by measuring the run-to-run variations in area from 30 pL injections of the various concentrations of microRNA, which were performed in triplicates and normalized by the area of the fluorescein internal standard.

The cell lysate was prepared in the following way: MCF-7 cells were purchased from ATCC and grown in incubator at 37°C in the atmosphere of 5% CO_2. Cells were grown in DMEM/F12 media (Invitrogen, Carlsbad, CA, USA) with 20 ng/mL hEGF, 0.5 μg/mL hydrocortisone, 10 μg/mL insulin, FBS and 10,000 μg/mL penicillin, streptomycin in a 100 mm Petri dish. When cells covered roughly 90% of the plate they were washed with PBS, trypsinized to be detached from bottom of dish and centrifuged at 150×g for 5 min. Pellet was washed twice with PBS. The cells were counted using haemocytometer and lysed with 1% Triton in 50 mM Tris-Acetate, 50 mM KCl, 10 μM masking RNA, 0.1 mM EDTA, pH 8.16. Cell lysates were aliquoted and stored in liquid nitrogen.